ADVANCED FUNCTIONAL MATERIALS
www.afm-journal.de

Materials Views
www.MaterialsViews.com

Universal Polarization Switching Behavior of Disordered Ferroelectrics

Yuri A. Genenko, Sergey Zhukov, Sergey V. Yampolskii, Jörg Schütrumpf, Robert Dittmer, Wook Jo, Hans Kungl, Michael J. Hoffmann, and Heinz von Seggern*

Universal scaling features of polarization switching are established experimentally in rather different classes of disordered ferroelectrics: in well-studied lead-zirconate titanate (PZT) ferroelectrics, in recently synthesized Cu-stabilized 0.94($Bi_{1/2}Na_{1/2}$)TiO_3–0.06$BaTiO_3$ (BNT-BT) relaxor ferroelectrics, and in classical organic ferroelectrics P(VDF-TrFE). These scaling properties are explained by an extended concept of an inhomogeneous field mechanism (IFM) of polarization dynamics in ferroelectrics. Accordingly, disordered ferroelectrics exhibit a wide spectrum of characteristic switching times due to a statistical distribution of values of the local electric field. How this distribution can be extracted from polarization measurements is demonstrated. Generally, it is shown that the polarization response is primarily controlled by the statistical characteristics of disorder rather than by a temporal law of the local polarization switching.

1. Introduction

Although field-induced switching of polarization in ferroelectrics is a key process for the functioning of many devices, its essential features still elude understanding. Global polarization reversal is described mostly in one of two ways: either as a uniform random nucleation of reversed domains according to the Kolmogorov–Avrami–Ishibashi (KAI) model[1–3] with a single field-dependent switching time τ or as a superposition of responses of numerous regions exhibiting independent switching kinetics,[4–8] characterized by a broad distribution of switching times $g(\tau)$. From the microscopic point of view, local polarization reversal proceeds by few universal mechanisms common for rather different ferroics.[9] These include polarization rotation or nucleation and expansion of reversed domains, which may occur in different regimes: creep, depinning, or a sliding motion of domain walls, depending on the driving field strength. Here, we demonstrate, by analyzing experiments, a similarity of global switching behavior in very different ferroelectric material classes, whose universal properties cannot be explained by using the KAI approach. We show, on the other hand, that the universal switching behavior can be readily explained by applying statistical concepts[10–12] whereby a certain law of local polarization switching does not play an essential role. Moreover, we show how the distribution of switching times is related to the statistical distribution of the local electric field values and how the latter can be directly extracted from experiment without any preliminary hypothesis on its specific shape.

The KAI model suggests the following temporal dependence of the reversed polarization

$$p(t,\tau) = 2P_s\left\{1-\exp\left[-\left(\frac{t}{\tau}\right)^{\beta}\right]\right\} \quad (1)$$

where t is the time elapsed after the application of the external field E, $2P_s$ is the amount of the reversed polarization reached at saturation, and β and τ are material parameters. In the classical KAI approach[1–3,13] the Avrami exponent β depends on the dimensionality of a domain nucleus and takes only integer values, however, common experimental practice is to consider both β and τ as arbitrary field-dependent fitting parameters. Such interpretation does not rely on any theoretical concept but resembles for the cases with $\beta < 1$[14–18] the fractional power relaxation law, often utilized to describe the response of dielectrics.[19]

For the other parameter τ an empirical law[20] is often used:

$$\tau(E) = \tau_0 \exp\left[\left(\frac{E_a}{E}\right)^{\alpha}\right] \quad (2)$$

with τ_0 the characteristic time, E_a the activation field, and α the constant adopting values around 1. Experimentally, Equation (2) is confirmed in numerous studies on single crystals,[20] bulk ceramics,[10–12,15] thin films,[4,6,8,17,18] and organic-ferroelectric composites.[7] Theoretically, the field dependence of the nucleation process was investigated by many authors[13,21–23] of which a dependence close to Equation (2) was derived for domain nucleation supported by tunneling of free charges for electric fields smaller than 0.1 kV mm^{-1}.[21]

Only verified in experiments on ferroelectric single crystals of triglycine sulphate,[24] the genuine KAI dependence in Equation (1) with integer β does not seem to hold for thin films,[4–6,8,25]

Dr. Y. A. Genenko, Dr. S. Zhukov, Dr. S. V. Yampolskii, J. Schütrumpf, R. Dittmer, Dr. W. Jo, Prof. H. von Seggern
Institut für Materialwissenschaft
Technische Universität Darmstadt
Darmstadt, 64287, Germany
E-mail: yugenen@tgm.tu-darmstadt.de
Dr. H. Kungl, Prof. M. J. Hoffmann
Institut für Angewandte Materialien–Keramik in Maschinenbau
Karlsruher Institut für Technologie
Karlsruhe, 76131, Germany

DOI: 10.1002/adfm.201102841

organic-ferroelectric composites,[7] and bulk polycrystalline samples.[10–12,15,26] The KAI function has, for any choice of parameters, a step-like shape on the logarithmic time scale that is nearly symmetric with respect to its inflection point. Polarization reversal reported in literature[4–8,12,15,25,26] exhibits non-symmetric curves with extended quasilinear tails on the logarithmic time scale, which cannot be fitted by a function such as Equation (1); hence, such systems cannot be described by a unique relaxation time τ. In the spirit of the Preisach model,[27] considering a ferroelectric sample as a collection of independent bistable units with distributed parameters,[28] the temporal response of a disordered system can be represented as that of an ensemble of elementary regions characterized by different switching times with a broad distribution of these times $g(\tau)$ covering many decades.[4]

Such distributions of switching and relaxation times were, in fact, observed by spatially resolved piezoresponse force microscopy on polycrystalline ferroelectric films[29] and bulk ferroelectric relaxors.[30] Broad time spectra were attributed to the distribution of activation energies U_a related to the relaxation time as $\tau = \tau_0 \exp(U_a/kT)$ with the Boltzmann constant k and temperature T. In conjunction with Equation (2), an expression of the energy barrier U_a through the local value of the electric field E in the form $U_a = U^* (E^*/E)^{\alpha}$ could be suggested, with U^* and E^* the constants, which ensues in turn the relation $E_a = E^* (U^*/kT)^{1/\alpha}$ for the activation field. These expected relations should still be proven by measurements in possibly wide temperature and field regions. Theoretically, these field and temperature dependences of the time τ are reminiscent of the theory of thermal creep of an elastic domain wall due to collective pinning by weak randomly distributed pinning centers.[31]

The hypothesis of the field-dependent activation barrier can simply explain the distribution of switching times in mesoscopically heterogeneous systems by the inhomogeneous field distribution in them, as was suggested in the inhomogeneous field mechanism (IFM) model of polarization reversal.[10–12] This idea, qualitatively discussed previously,[15] was first quantitatively implemented in ref. [6,7] where the statistical distribution of values of the local electric field in thin ferroelectric films was modelled as a Lorentzian curve. On the other hand, for the virgin, as-prepared lead-zirconate titanate (PZT) bulk ceramics, this distribution can also be satisfactorily fitted by a Gaussian function.[11] As will be shown below, it is not necessary to assume any certain form of the field distribution since it can be extracted directly from experiment.

In previous applications of the IFM concept to bulk ferroelectric ceramics[10–12] the angle dependence of the local electric field was neglected similarly to the case of thin films,[4,6,7] which is a poor approximation. In the 3D case, the Maxwell equation $\nabla(\hat{\varepsilon}\mathbf{E}) = 0$ holds inside a bulk dielectric, where $\hat{\varepsilon}$ is a dielectric permittivity tensor. This means that the component of the electric field parallel to the applied field direction can only change when the perpendicular field components change to the same extent, assuming the permittivity tensor to be macroscopically isotropic. Thus, a distribution of the values of the local electric field in 3D solids implies inevitably a distribution of the field orientations. Therefore, in the following Section 2, we present an extended IFM model taking into account the angle dependence of the local fields and then, in Section 3, compare predictions of this model with experiments performed on different classes of ferroelectrics. Finally, the results are summarized and discussed in Section 4. Additional details on materials and experimental procedures are given in the Experimental Section and in Supporting Information.

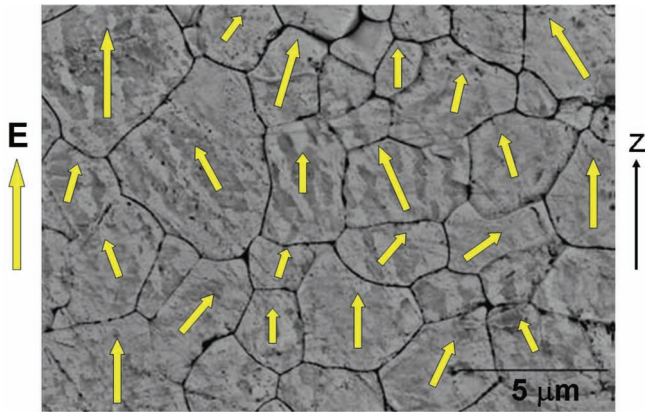

Figure 1. Scheme of an inhomogeneous field distribution in a ferroelectric ceramic. A scanning electron microscopy image of a PZT sample is used as a background.

2. Extension of the IFM Model of Polarization Switching

We consider 3D disordered ferroelectrics composed of anisotropic regions (grains) that are distributed and oriented arbitrarily in space (**Figure 1**). The following polarization switching scenario is imposed: the system is first polarized for a long time by an applied electric field much higher than its coercive field, then short circuited for an extended time and consequently the field is applied into the opposite direction and switching is observed. As mentioned above, in this model the statistical distribution of switching times of different regions $g(\tau)$ is determined by the statistical distribution of local electric field values E through an arbitrary relation $\tau(E)$. If the considered disordered system is macroscopically homogeneous, isotropic and not textured, then the statistical distribution function for the electric field vector $W(\mathbf{E})$ in the field space becomes cylindrically symmetrical with respect to the direction of the applied field $\mathbf{E}_m$. We assume additionally that the system is characterized by a permittivity tensor $\hat{\varepsilon}$ which may spatially vary but is field-independent. This means that the local field resulting from the spatial redistribution of the external field scales at every point with the value of the applied field E_m. Then the statistical distribution of the local field vectors in the spherical coordinate frame (E,ϕ,θ) can be reduced to the function $F(E/E_m,\theta)$ defined by the relation

$$F\left(\frac{E}{E_m},\theta\right)\frac{dE}{E_m} = \int_0^{2\pi} d\varphi \int_{E<|\mathbf{E}|<E+dE} d|\mathbf{E}|\,|\mathbf{E}|^2\,W(\mathbf{E}) \qquad (3)$$

where ϕ and θ are the azimuthal and polar angle of the local field with respect to the applied field direction z, respectively.

According to its statistical meaning this distribution function is obviously normalized:

$$\int_0^\infty \mathrm{d}s \int_0^\pi \mathrm{d}\theta \sin\theta F(s,\theta) = 1 \tag{4}$$

with $s = E/E_\mathrm{m}$ the normalized electric field. One more normalization condition arises from the fact that the mean electric field in the direction of the applied field, $<E_z>$, should be equal to E_m:

$$\int_0^\infty \mathrm{d}s s \int_0^\pi \mathrm{d}\theta \sin\theta \cos\theta F(s,\theta) = 1 \tag{5}$$

The distribution of switching times can be restored from the distribution of fields using the relation

$$g(\tau)\,\mathrm{d}\tau = (\mathrm{d}E/E_\mathrm{m}) \int_0^\pi \mathrm{d}\theta \sin\theta F(E/E_\mathrm{m},\theta) \tag{6}$$

if the field dependence of the switching time $\tau(E)$ is known and applies in the whole volume of the system. From a physical point of view, the time τ may change between 0 and ∞ because the switching mechanism is not exactly known. On the other hand, when using for $\tau(E)$ the dependence in Equation (2), it should be noted that the lowest switching time possible is not zero but τ_0. This, however, should not lead to an error since the involved measurement durations t of more than 10^{-6} s are by orders of the magnitude larger than typical values of τ_0.

In contrast to usual model considerations of thin films,[4–8] in bulk samples the local polarization may switch in different directions depending on the local field and crystal axes orientations. We assume for simplicity that the polarization switches to the direction of the local field and, thus, the contribution to the total polarization in the applied field direction is proportional to $p[t,\tau(E)]\cos\theta$. Herewith the parameter P_s in Equation (1) should be reduced with respect to the corresponding single crystal values: in perovskite single crystals by a factor of 0.831 in the tetragonal case and by a factor of 0.866 in the rhombohedral case,[32] in polyvinylidene difluoride (PVDF) ferroelectrics by a factor of $3/\pi$.[33] Then, similarly to the nucleation limited switching (NLS) model of ferroelectric films,[4] the polarization response of the highly polarized bulk ferroelectric medium to the reversed external field E_m may be presented as a superposition of local KAI-like responses,

$$\Delta P(E_\mathrm{m},t) = \int_0^\infty \mathrm{d}s \int_0^\pi \mathrm{d}\theta \sin\theta\cos\theta F(s,\theta)\, p[t,\tau(E_\mathrm{m}s)] \tag{7}$$

Maximum value of the local polarization in Equation (1) reached asymptotically at $t \to \infty$ is $2P_\mathrm{s}$. This results in the maximum value of the total switched polarization

$$\begin{aligned}\Delta P_\mathrm{max} &= 2P_\mathrm{s} \int_0^\infty \mathrm{d}s \int_0^\pi \mathrm{d}\theta \sin\theta\cos\theta F(s,\theta) \\ &= 2P_\mathrm{s} <\cos\theta>\end{aligned} \tag{8}$$

where $<\cos\theta>$ as a characteristic of the average orientation of the local polarization was introduced.

The double exponential dependence in the function $p[t,\tau(E)]$ of Equation (7) results in the step-like dependence on the field E or on time t (on logarithmic scale), which looks very much like the Heaviside unit step function: $p(t,\tau) \approx 2P_\mathrm{s}H(t-\tau)$, especially when $\beta > 1$. This allows one to roughly approximate the function $p[t,\tau(E)]$ by $2P_\mathrm{s}H[E - E_\mathrm{th}(t)]$, where $E_\mathrm{th}(t)$ is the solution of the equation $\tau(E) = t$, and to perform a truncation of integration in Equation (7) resulting in an approximate form

$$\begin{aligned}\Delta P(E_\mathrm{m},t) &\approx 2P_\mathrm{s} \int_{E_\mathrm{th}/E_\mathrm{m}}^\infty \mathrm{d}s \int_0^\pi \mathrm{d}\theta \sin\theta\cos\theta F(s,\theta) \\ &= \Delta P_\mathrm{max} \int_{E_\mathrm{th}/E_\mathrm{m}}^\infty \mathrm{d}s f(s)\end{aligned} \tag{9}$$

Here a weighted distribution function for normalized field values was introduced as

$$f(s) = \frac{1}{<\cos\theta>} \int_0^\pi \mathrm{d}\theta \sin\theta\cos\theta F(s,\theta) \tag{10}$$

which generalizes the statistical distribution of field values in ref. [12], where explicit angle dependence was not accounted for. By integrating this function over s one finds that, according to Equation (8), it is normalized:

$$\int_0^\infty \mathrm{d}s f(s) = 1 \tag{11}$$

Besides, by multiplying Equation (10) with s and integrating over s, Equation (5) can be used to find another normalization condition

$$\int_0^\infty \mathrm{d}s s f(s) = \frac{1}{<\cos\theta>} \tag{12}$$

which is slightly different from one in ref. [12], where the angle distribution of the field was missing.

According to the approximate representation in Equation (9) the polarization response is expected to exhibit, similarly to ref. [12], certain scaling properties. Indeed, $\Delta P(E_\mathrm{m},t)$ appears to be a function of a combined field and time variable $E_\mathrm{m}/E_\mathrm{th}(t)$ only. Moreover, it becomes possible to directly extract the distribution function $f(s)$ from the switched polarization. Namely, its normalized logarithmic derivative with respect to the applied field acquires a scaling form

$$\frac{1}{\Delta P_\mathrm{max}} \frac{\partial \Delta P(E_\mathrm{m},t)}{\partial \ln E_\mathrm{m}} = \frac{E_\mathrm{th}(t)}{E_\mathrm{m}} f\left(\frac{E_\mathrm{th}(t)}{E_\mathrm{m}}\right) \tag{13}$$

The right-hand side of this equation is a function of the mentioned combined variable $E_\mathrm{m}/E_\mathrm{th}(t)$, hence, the left-hand side must also be a function of such a variable. All logarithmic derivatives exhibit a maximum at some time-dependent position $E_\mathrm{max}(t)$. Equation (13) means that logarithmic derivatives for different poling times t have to be of the same height at their maximum positions and scale to the same master curve $\Phi[E_\mathrm{m}/E_\mathrm{max}(t)]$, which presents a fingerprint of the system. Thereby $E_\mathrm{max}(t) = \gamma E_\mathrm{th}(t)$ must hold, with γ a constant. Finally, Equation (13) allows explicit determination of the distribution function $f(s)$ from the above master curve as

$$f(s) = \frac{1}{s}\Phi\left(\frac{1}{\gamma s}\right) \tag{14}$$

The constant γ is not arbitrary and can be found by substitution of Equation (14) into Equation (12), which results in the relation

$$\gamma = <\cos\theta> \int_0^\infty \frac{du}{u^2}\,\Phi(u) \qquad (15)$$

deriving this constant from the form of the master curve $\Phi(u)$ and the average polarization orientation. The other normalization condition, Equation (11), is satisfied for arbitrary γ by substitution of Equation (14) due to the fact that $\Delta P(E_m,t)$ saturates by the value ΔP_{max} at infinite E_m for arbitrary t.

The above analysis allows to a large extent the determination of the weighted statistical distribution of the local electric field values, Equation (10), leaving, however, the angle distribution of the local fields hidden because the measurable total polarization, Equation (7), averages local vectorial contributions over the whole system. The only trace of the angle dependence is the average orientation <cos θ> appearing in Equation (15). The latter parameter can only be roughly estimated if the maximum possible polarization for a certain material, P_s, is known from independent measurements. In this case <cos θ> can be valuated as $\Delta P_{max}/2P_s$ according to Equation (8).

Fortunately, the above uncertainty in the determination of the parameter γ and consequently of the distribution function $f(s)$ has no effect on the evaluation of the total polarization response, Equation (9). Indeed, by substitution of Equation (14) into Equation (9) one obtains a simple expression

$$\Delta P(E_m, t) = \Delta P_{max} \int_0^{E_m/E_{max}} \frac{du}{u}\,\Phi(u) \qquad (16)$$

relating the reversed polarization directly to the measurable quantities: the master curve $\Phi(u)$ and the maximum position $E_{max}(t)$.

Although validity of Equation (13) has been largely confirmed on virgin and fatigued PZT materials[12] the question remains if neglecting the details of the local polarization reversal by introducing the step function instead of $p[t,\tau(E)]$ is well enough justified. Indeed, this model assumption allowing for truncation of the integration in Equation (7) and consequently leading to Equation (13) completely ignores the temporal behavior of the local polarization by assuming simply that the local switching occurs instantly when the observation time reaches the local value of the characteristic time $\tau(E)$. We now investigate the effect of the elementary switching process on the overall response of the ferroelectric medium assuming that the local switching is controlled by Equations (1) and (2) with arbitrary parameters involved.

To this end we calculate the logarithmic derivative of Equation (7) and obtain

$$\frac{1}{\Delta P_{max}}\frac{\partial \Delta P(E_m,t)}{\partial \ln E_m} = \int_0^\infty ds\, s f(s)\, D(s)$$

$$\text{with } D(s) = \frac{E_m}{2P_s}\left(\frac{\partial p}{\partial \tau}\frac{\partial \tau}{\partial E}\right)\Big|_{E/E_m=s} \qquad (17)$$

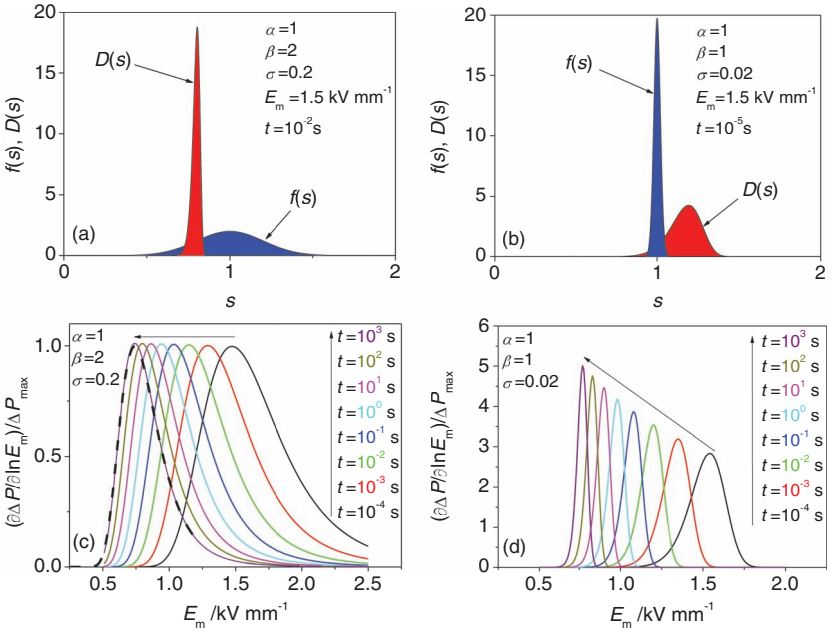

Figure 2. Model field derivative of the local polarization $D(s)$ and the distribution function $f(s)$ for the cases when this distribution is a) much wider and b) much more narrow than the derivative peak. c) Model calculations of the logarithmic field derivative, Equation (17), for the case in (a). d) The same calculations for the case in (b).

The integrand presents a product of two peak functions, the second of which, $D(s)$, was, in fact, substituted by the Dirac delta function $\delta(s - E_{th}/E_m)$ by the derivation of Equation (13). If, in contrast, the field distribution $f(s)$ were assumed to be $\delta(s-1)$, that corresponds to the uniform field in the whole system, the total polarization, Equation (7), would be reduced to Equation (1). It is easy to check that in this case the scaling property of the logarithmic derivative, Equation (13), would not hold. To illustrate this fact, we display in **Figure 2** exemplary calculations of Equation (17) for two opposite cases using different parameters involved in expressions for $p(t,\tau)$ and $\tau(E)$ given by Equations (1) and (2), respectively. For the parameters chosen in Figure 2a, the width of the derivative $D(s)$ is much less than the width $\sigma = 0.2$ of the normal Gaussian distribution taken for the function $f(s)$. Corresponding logarithmic derivatives shown in Figure 2c all scale to the only curve, which is demonstrated by scaling of the widest curve to the dashed line coinciding with the narrowest curve. For the parameters chosen in Figure 2b, the width of the derivative $D(s)$ is much larger than the width $\sigma = 0.02$ of the Gaussian distribution taken for the function $f(s)$. Corresponding logarithmic derivatives shown in Figure 2d exhibit maxima rising with the increasing observation time t, which makes scaling to the same master curve impossible. Transition between the two opposite cases is continuous, which may be observed by changing the relevant parameters indicated in Figure 2a,b. Thus, the scaling relation, Equation (13), serves as a criterion for validity of the IFM model for a given material. If scaling is fulfilled then disorder dominates the polarization switching, if it fails then the system reacts as an effectively homogeneous medium.[24]

To establish when Equation (13) is expected to be valid in terms of parameters involved we now evaluate the integral in

Equation (17) beyond the δ-function approximation for $D(s)$. This can be performed in the spirit of Laplace's method[34] assuming that $f(s)$ behaves smoothly near the sharp maximum of $D(s)$. Position of the latter maximum and its width are given by expressions

$$s_0 = \frac{E_a}{E_m}\frac{\alpha}{\ln(t/\tau_0)} \text{ and } w = \frac{s_0}{\beta \ln(t/\tau_0)} \qquad (18)$$

respectively. If a condition of the peak sharpness, $w << s_0$, that is equivalent to $\beta \ln(t/\tau_0) >> 1$, is fulfilled, and s_0 is far away from the maximum of the function $f(s)$, which is typically around 1, Equation (17) can be evaluated as $\left(\sqrt{2\pi}/e\right) s_0 f(s_0)$, that is nearly the same as in the δ-function approximation for $D(s)$. The required inequality $\beta \ln(t/\tau_0) >> 1$ is typically satisfied since the values of $\ln(t/\tau_0)$ lie between 4 and 33 for t from the interval $(10^{-5},10^{2})$ s and τ_0 from the interval $(10^{-13},10^{-7})$ s, when the integer β is taken.[1–3,5,24] If, in contrast, $s_0 \approx 1$ is realized, then the ratio $w/D(s_0) \approx [\beta \ln(t/\tau_0)]^{-2} << 1$ holds, which again warrants the δ-function approximation for $D(s)$ provided that the width of $f(s)$ is larger than w. This seems to be the case already for the virgin PZT materials[11] and even more so for fatigued ones.[12] Thus, it is to be expected that the scaling relation, Equation (13), holds for a wide class of disordered ferroelectrics.

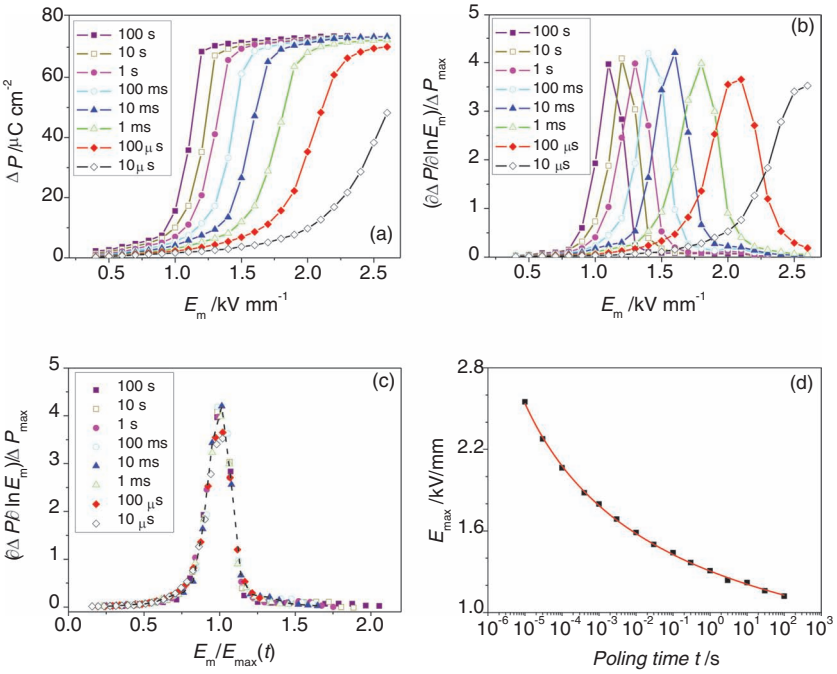

Figure 3. a) Switched polarization of PZT ceramic ΔP as a function of applied field E_m at different poling times t as indicated, b) its logarithmic derivatives versus applied field, c) the same derivatives scaled to their maximum positions $E_{max}(t)$, and d) fitting of $E_{max}(t)$ with an inverse logarithmic function.

3. Experimental Verification

The above discussed scaling properties will now be experimentally verified on three different systems: PZT ceramic-$Pb_{0.975}Sr_{0.02}[(Zr_{0.5225}Ti_{0.4775})_{0.99}Nb_{0.01}]O_3$,[35] Cu-stabilized BNT-BT ceramic $0.94(Bi_{1/2}Na_{1/2})TiO_3$–$0.06BaTiO_3$,[36] and classical organic ferroelectric 70/30 mol% copolymer of vinylidene-fluoride and trifluoroethylene P(VDF-TrFE).[37,38] All the measurements were done at room temperature using equipment and procedures described below in Section 5. The polarization response was measured in the time window between 10^{-6} s and 10^{2} s for a set of E_m values varied in between $\approx 0.3E_C$ and $\approx 3E_C$, where E_C is the coercive field for the respective material. Then the switched polarization ΔP was represented as a function of E_m for different poling durations and the derivative in Equation (13) was computed.

This study was first carried out on a series of the above mentioned polycrystalline PZT ceramics, prepared as cylindrical pellets with 10 mm in diameter and 1 mm in thickness and sintered at different temperatures between 975 and 1100 °C so that they possessed different average grain sizes between 1 and 3 μm.[35] All materials investigated revealed large fractions of tetragonal crystal structure defined by the chosen composition on the tetragonal side of the morphotropic phase boundary (see Figure S3 in Supporting Information). Though PZTs with different grain sizes reveal different domain structures and consequently diverse polarization dynamics[5,35] all the samples studied exhibited similar scaling features. As an example, the results for the ceramic sintered at 975 °C and possessing the average grain size of 1.06 μm are presented in **Figure 3** (see also Figure S2a in Supporting Information). Logarithmic derivatives reach roughly the same level at maximum as is seen in Figure 3b and can be scaled to the same master curve as displayed in Figure 3c. Hence, in accordance with Equation (13), a ratio $E_{max}(t)/E_{th}(t) = \gamma$ remains constant. The parameter $<\cos\theta> = \Delta P_{max}/2P_s$ can be roughly estimated as 0.817 by taking for P_s the maximum saturation polarization value of 45 μC cm^{-2}, known for this material in the form of bulk samples or thin films,[39] assuming that by this value a virtually uniform field distribution is realized. Then the parameter γ can be derived from Equation (15). Dependence of the maximum position E_{max} on the poling time t can be well fitted by the function $E_0/[\ln(t/\tau_0)]^{1/\alpha}$ as is shown in Figure 3d. This means that the relation (2) is valid with $E_a = E_0/\gamma$ for a wide interval of poling times utilized. E_0, α, and τ_0 values obtained from the above fit and the other IFM model parameters are presented in **Table 1**.

Numerically restored from the master curve $\Phi[E_m/E_{max}(t)]$ (see Figure 3c) using Equation (14) the distribution function $f(E/E_m)$ is depicted in **Figure 4**a, while Figure 4b relates the resulting IFM model calculations according to Equation (16) (solid lines) to the experimental data shown by symbols. Note an asymmetric form of the distribution function in Figure 4a, which can hardly be fitted by a Lorentzian function as suggested in ref. [6–8].

Another investigated example of perovskite ferroelectrics, the Cu-stabilized BNT-BT ceramic samples were prepared by a procedure described in ref. [36] as pellets of about 7.2 mm in diameter and 300 μm in thickness and possessed average

Table 1. The IFM-model parameters for different materials described in the text.

sample	ΔP_{max} [μC cm^{-2}]	E_0 [kV mm^{-1}]	α	τ_0 [s]	<cos θ>	γ
PZT	73.5	8.22 ± 0.75	1.56 ± 0.07	(1.85 ± 0.04) × 10^{-8}	0.817	0.903
BNT-BT	77.5	528.8 ± 6.8	0.65	(2.95 ± 0.58) × 10^{-13}	0.829	0.858
P(VDF-TrFE)	16.2	291.5 ± 34.2	1.67 ± 0.10	(2.70 ± 1.23) × 10^{-7}	0.848	0.808

grain size of 1 μm (see Figure S2b in Supporting Information). BNT-BT is one of the most widely studied lead-free piezoceramics owing to its comparably good electromechanical properties and a number of peculiar features.[40,41] Similar to PZT, BNT-xBT exhibits a morphotropic phase boundary where electrical properties peak. This boundary is at x = 6% between the rhombohedral BNT and the tetragonal BT. However, other than PZT, BNT-6BT is believed to be a relaxor ferroelectric that shows a field-induced transition from relaxor to long-range order state.[42] The BNT-6BT composition studied here at room temperature revealed predominantly rhombohedral crystal structure with some tetragonal phase present (see Figure S4 in Supporting Information) which both remained stable over the whole field range investigated. As well as in the case of PZT materials the logarithmic field derivatives of the switched polarization could be scaled to the same master curve as displayed in **Figure 5**a. From this scaling procedure the dependence of the maximum position E_{max} on the poling time t was obtained and fitted by the function $E_0/[\ln(t/\tau_0)]^{1/\alpha}$ as is shown in Figure 5b. Equation (2) was again valid in the whole region of the fields and poling times utilized with $E_a = E_0/\gamma$. Taking $P_s = 54$ μC cm^{-2} value from single crystal data for this material[43] reduced by the factor 0.866, the average orientation of the local polarization <cos θ> = 0.829 may be roughly estimated. Together with the master curve this parameter allows evaluation of the parameter γ using Equation (15). Numerically restored from the master curve, Figure 5a, using Equation (14) the distribution function $f(E/E_m)$ is depicted in Figure 5c, while Figure 5d shows calculations with Equation (16) by solid lines and the respective experimental data by symbols.

The same analysis was applied to the experimental data for the ferroelectric copolymer P(VDF-TrFE) provided by PiezoTech S.A.S. (France) as 9 μm thick films. Model parameters obtained in the same manner as above are summarized in Table 1 assuming the maximum polarization known for this composition[33] about $P_s = 10$ μC cm^{-2} reduced by the factor $3/\pi$, which entails <cos θ> = 0.848. The scaled logarithmic derivatives, the fitting of their maximum positions, the distribution function $f(E/E_m)$ and resulting temporal dependences of polarization are displayed in **Figure 6**a–d, respectively. The scaling relation, Equation (13), is well confirmed experimentally also in this class of ferroelectric materials exhibiting very different polarization reversal mechanisms,[38,44] namely, rotation of CH_2–CF_2 and CHF–CF_2 dipoles about the C–C main chain with domain wall progressing via molecular chain rotations in contrast to the deformation of a crystal cell in PZT and BNT-BT.

We notice a diversity of the parameters E_0, α and τ_0 characterizing different materials in Table 1. τ_0 is usually interpreted as the characteristic time of some microprocess relevant to ferroelectricity as, for example, the inverse of the soft-mode frequency ≈10^{-13} s,[4] but it was also interpreted as the inverse depinning frequency for domain walls of ≈10^{-11} s[9] or of ≈10^{-6} s.[45] E_0 is comparable with the activation field E_a, which is expected to have an upper limit in the thermodynamic coercive field of about 100 kV mm^{-1}.[4] The exponent α has no clear physical meaning, its reported values being around 1 in ref. [6–8,20,26] and between 1 and 2.5 in ref. [4,46]. If the domain wall creep[31] is assumed as the most likely mechanism of polarization reversal in the studied field-time region, which is advisable observing validity of Equation (2), then drastic differences in E_0 and τ_0 may be understood due to different pinning conditions and fragmentation of domain walls during the creep motion in the classical ferroelectric PZT and in the relaxor ferroelectric BNT-BT. Another remarkable feature is the extremely wide dispersion of the fitting parameters for the latter material. Formally it is a consequence of the weak dependence of the fitting function $E_0/[\ln(t/\tau_0)]^{1/\alpha}$ on E_0 and τ_0, particularly, when α becomes small. This renders comparably good fitting of the experimental data for $E_{max}(t)$ for rather different parameter sets. To reduce this multiplicity we have chosen from all values delivering a good data fitting the value of the exponent α as close as possible to unity and optimize the other two parameters resulting in numbers shown in Table 1.

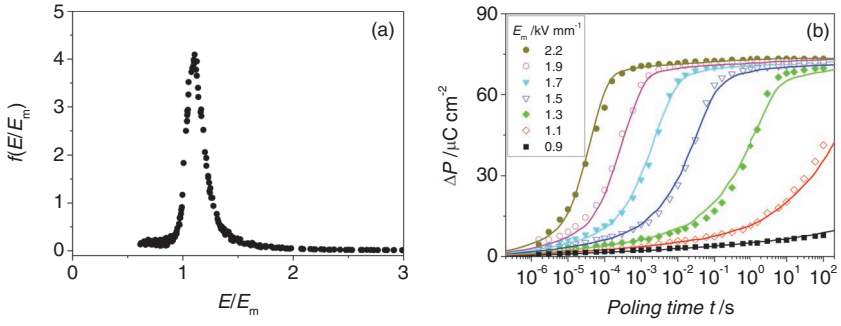

Figure 4. a) The weighted statistical distribution of the local field values $f(E/E_m)$ in PZT as extracted from Equation (14). b) Representation of the time dependent polarization reversal in PZT for different applied fields E_m with Equation (16) and respective experimental data shown by symbols.

4. Discussion and Conclusions

Three above considered examples of rather different ferroelectrics are well described by the IFM concept in spite of obvious diversity of microscopic mechanisms of polarization in them. In our statistical approach these mechanisms contribute in two issues: in a local polarization switching law $p(t,\tau)$ and in a field dependence of the local switching time $\tau(E)$. If the statistical distribution of (normalized) field values $f(s)$ is much wider

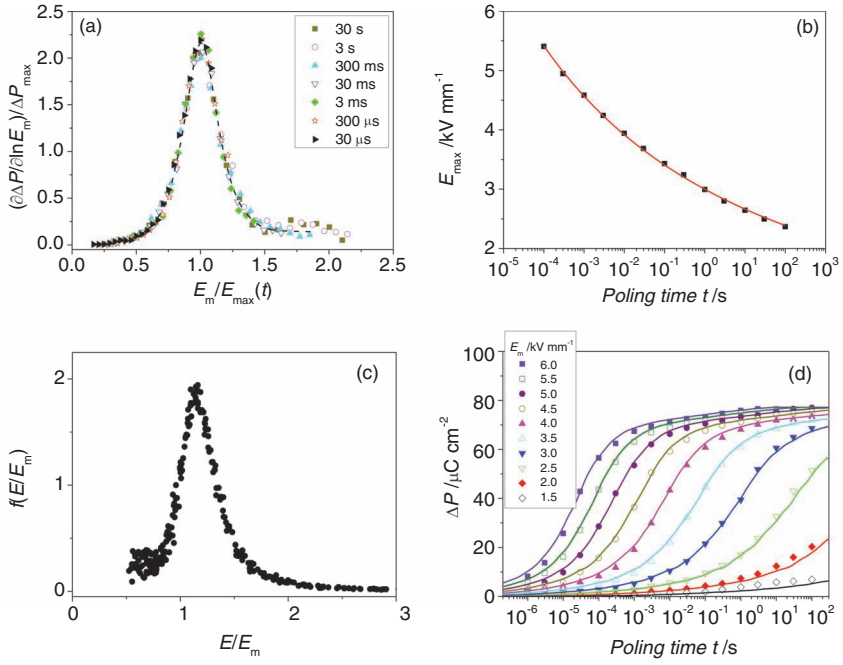

Figure 5. a) The master curve $\Phi[E_m/E_{max}(t)]$ resulting from scaling of logarithmic derivatives of the switched polarization to their maximum positions $E_{max}(t)$ in BNT-6BT at different poling times t as indicated. b) Fitting of $E_{max}(t)$ with an inverse logarithmic function. c) The distribution function $f(E/E_m)$ derived from $\Phi[E_m/E_{max}(t)]$ using Equation (14). d) Time dependent polarization reversal in BNT-6BT for different applied fields E_m evaluated with Equation (16) (solid lines) and respective experimental data shown by symbols.

than the dimensionless field derivative of $p(t,\tau)$ then the details of the local switching become unimportant for the total response. This is the case in all disordered ferroelectrics studied by us whatever the microscopic mechanism of switching they possess. On the other hand, the dependence $\tau(E)$ still bares witness to a certain microscopic mechanism at work. Unlike the NLS model,[4] the IFM concept does not assume a priori a certain mechanism (e.g., nucleation) of local polarization reversal so that $\tau(E)$ may adopt different forms.[9] The fact that this dependence remains the same in the whole time-field domain investigated is in favor of a unique switching mechanism dominating polarization reversal in our experiments, which is most likely creep of domain walls.[31] Though particularly in PVDF family of ferroelectrics the domain wall scenario of polarization switching seems questionable,[47] the present consensus is that switching in these materials does involve domain walls at least at applied fields not much larger than the relevant coercive field.[48,49]

Thus, irrelevant to a specific microscopic mechanism behind the local polarization switching the total polarization response appears to be determined by some weighted statistical distribution of the local electric fields values (Equation (10)) if a system is well disordered. This distribution can be determined from a master curve resulting in turn from the scaling of logarithmic field derivatives of the total polarization. The scaling property of the latter serves itself as the validity criterion for applicability of the IFM model to a certain system. Note that the genuine distribution function of switching times $g(\tau)$, Equation (6), is determined by the complete distribution function of fields $F(s,\theta)$, Equation (3), which cannot be extracted from the polarization response (Equation (7)) alone. Accordingly, $g(\tau)$ cannot be derived from the weighted distribution function $f(s)$. On the other hand, the total response of a system, Equation (7), can still be represented as

$$\Delta P(E_m, t) = \int_0^\infty d\tau\, Q(\tau)\, p(t,\tau) \tag{19}$$

where a weighted distribution function of switching times was introduced as

$$Q(\tau) = \frac{1}{E_m}\left|\frac{d\tau}{dE}\right|^{-1} f\left(\frac{E}{E_m}\right) \tag{20}$$

which can be directly derived from $f(s)$. Thus, Equation (19), used for description

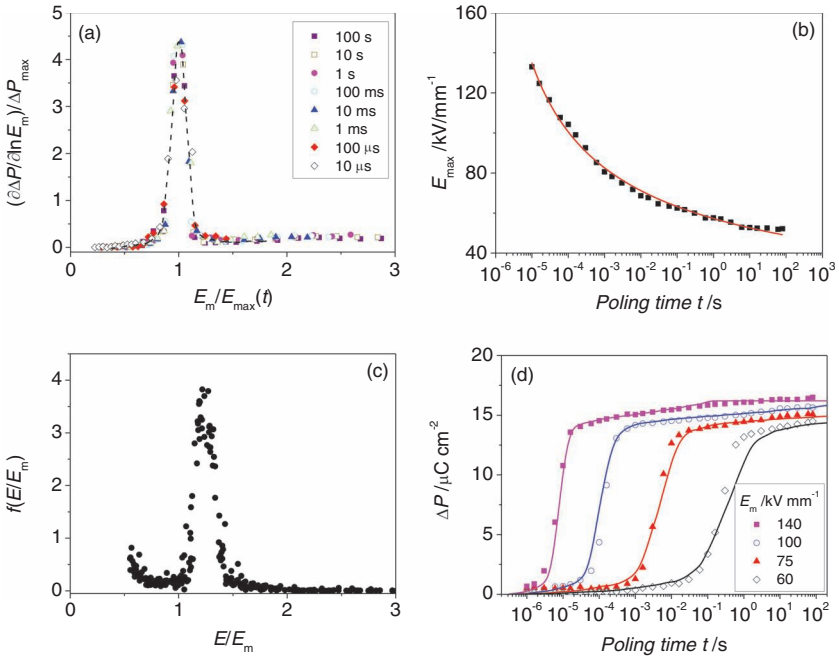

Figure 6. a) The master curve $\Phi[E_m/E_{max}(t)]$ resulting from logarithmic derivatives of the switched polarization versus field scaled to their maximum positions $E_{max}(t)$ in P(VDF-TrFE) at different poling times t as indicated. b) Fitting of $E_{max}(t)$ with an inverse logarithmic function. c) The distribution function $f(E/E_m)$ derived from $\Phi[E_m/E_{max}(t)]$ using Equation (14). d) Time dependent polarization reversal in P(VDF-TrFE) for different applied fields E_m evaluated with Equation (16) (solid lines) and respective experimental data shown by symbols.

of polarization response of thin ferroelectric films,[4,6,8] is applicable also to bulk ferroelectrics,[10–12] however, the distribution function of times used in this formula is not the genuine distribution, Equation (6), but the weighted one, Equation (20).

The relevance of the observed universal features of polarization switching to the universal frequency response of different ferroics owing to the statistical distribution of pinning forces[9] has to be further investigated, because, in contrast to the IFM case, quenched local random fields considered in ref. [9,50] are not supposed to scale with the external field. The same remark concerns also random electric fields induced by dilute, randomly distributed and randomly aligned dipoles considered in ref. [6,51] predicting for the local fields the Lorentzian and "square of Lorentzian" statistical distributions, respectively. Both distributions are characterized by half-widths independent of the external field and, hence, do not agree with the scaling of this width proportionally to the applied field observed in our experiments.

In conclusion, we have demonstrated that the polarization response of rather different disordered ferroelectrics is predominantly determined by the statistical characteristics of the disordered materials as opposed to the local switching dynamics. This statement, however, may be valid far beyond the area of ferroelectrics since the scenario of field-assisted polarization reversal seems to be common for wide classes of disordered media including ferromagnetics, ferroelectrics, ferroelectric relaxors and other ferroics.[31,50,52]

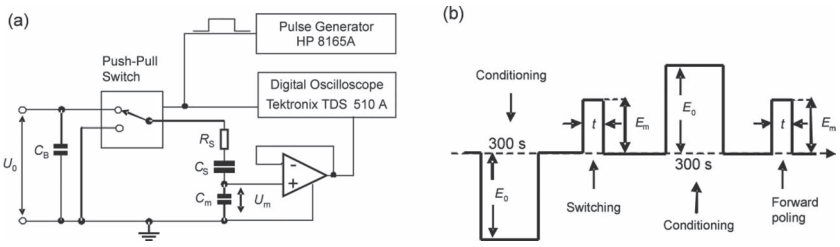

Figure 7. a) Schematic diagram of the experimental setup for measuring the polarization reversal. b) Pulse sequence utilized to measure the reversed polarization after application of the field E_m during the time t. During switching and forward cycles the temporal evolution of electrical displacement is recorded. The switched polarization $\Delta P(t)$ is calculated as difference between switching and forward poling displacement values taken at time t after application of the step voltage pulse.

5. Experimental Section

The PZT and BNT-BT samples were electroded with silver paste fired at 600 °C. For polymer samples electrodes of 50 nm thick gold and 0.5 cm in diameter were evaporated on both sides by physical vapour deposition.

For measurements of the switched polarization ΔP as a function of the applied electric field E_m for definite time t a pulse switching method was employed using an electrical circuit displayed in **Figure 7**a. A high voltage/high current push-pull switch from Behlke Co. (Germany) including a buffer 1 μF capacitor C_B as a voltage source was used to provide the voltage step U_0 up to 3 kV. The pulse duration from 1 μs to 100 s was controlled by a programmable signal source (Model 8165A from Hewlett Packard). The temporal evolution of the electric displacement in the sample C_s was detected by a sensing capacitor C_m = 4.4 μF connected in series with the current limiting resistor R_s of 100 Ω. The voltage drop U_m across the series capacitor was registered by means of a digital oscilloscope (Tektronix TDS 510 A) connected via a high impedance amplifier. The RC time constant of the experimental setup about 100 ns was shorter than the actual ferroelectric switching time of the investigated ferroelectric materials and shorter than the shortest voltage pulse (1 μs) applied in this study.

To investigate the polarization switching phenomenon, the samples were at first poled by applying the negative DC field of $E_0 \approx 2E_C$ for 300 s assuring that the maximum saturated polarization, $-P_s$, was reached after such poling procedure. A schematic diagram of the pulse sequence is shown in Figure 7b. After complete poling in the negative field direction, the positively directed switching field E_m was applied to the sample during definite time t. After switching experiment the sample was conditioned again, as shown in Figure 7b, to restore its $+P_s$ state by applying a positive field $E_0 \approx 2E_C$ for 300 s. At the forth step, forward poling was performed by applying the field E_m to the conditioned sample in the same direction for the time t (see Figure 7b). Since the sample was already polarized to its saturation at $+P_s$, the apparent displacement during forward poling contained all those components that existed in the switching experiment except for the switched ferroelectric polarization ΔP. Therefore, the switched polarization ΔP was determined as the difference between the displacement values of switching and forward poling taken at time t after application of the step voltage pulse. The applied fields E_m covered the range from $0.3E_C$ to $3E_C$, while the duration of the switching pulse t was varied in the wide time domain from 1 μs to 100 s.

Supporting Information

Supporting Information is available from the Wiley Online Library or from the author.

Acknowledgements

This work was supported by the Deutsche Forschungsgemeinschaft through the Sonderforschungsbereich 595 "Electrical Fatigue in Functional Materials".

Received: November 23, 2011
Revised: January 20, 2012
Published online: March 5, 2012

[1] A. N. Kolmogorov, *Izv. Akad. Nauk, Ser. Math.* **1937**, *3*, 355.
[2] M. Avrami, *J. Chem. Phys.* **1940**, *8*, 212.
[3] Y. Isibashi, *Ferroelectrics* **1989**, *98*, 193.
[4] A. K. Tagantsev, I. Stolichnov, N. Setter, J. S. Cross, M. Tsukada, *Phys. Rev. B* **2002**, *66*, 214109.
[5] A. Gruverman, B. J. Rodriguez, C. Dehoff, J. D. Waldrep, A. I. Kingon, R. J. Nemanich, *Appl. Phys. Lett.* **2005**, *87*, 082902.
[6] J. Y. Jo, H. S. Han, J.-G. Yoon, T. K. Song, S.-H. Kim, T. W. Noh, *Phys. Rev. Lett.* **2007**, *99*, 267602.
[7] A. Nautiyal, K. C. Sekhar, N. P. Pathak, N. Dabra, J. S. Hundal, R. Nath, *Appl. Phys. A* **2010**, *99*, 941.
[8] N. Dabra, J. S. Hundal, A. Nautiyal, K. C. Sekhar, R. Nath, *J. Appl. Phys.* **2010**, *108*, 024108.
[9] W. Kleemann, *Annu. Rev. Mater. Res.* **2007**, *37*, 415.
[10] S. Zhukov, S. Fedosov, J. Glaum, T. Granzow, Y. A. Genenko, H. von Seggern, *J. Appl. Phys.* **2010**, *108*, 014105.
[11] S. Zhukov, Y. A. Genenko, H. von Seggern, *J. Appl. Phys.* **2010**, *108*, 014106.

[12] S. Zhukov, Y. A. Genenko, O. Hirsch, J. Glaum, T. Granzow, H. von Seggern, *Phys. Rev. B* **2010**, *82*, 014109.
[13] M. Vopsaroiu, J. Blackburn, M. G. Cain, P. M. Weaver, *Phys. Rev. B* **2010**, *82*, 024109.
[14] C. Verdier, D. C. Lupascu, H. von Seggern, J. Rödel, *Appl. Phys. Lett.* **2004**, *85*, 3211.
[15] D. C. Lupascu, S. Fedosov, C. Verdier, J. Rödel, H. von Seggern, *J. Appl. Phys.* **2004**, *95*, 1386.
[16] J. Li, Y. Zhang, H. Cai, X. Yi, *J. Electroceram.* **2010**, *25*, 135.
[17] D. Pantel, Y.-H. Chu, L. W. Martin, R. Ramesh, D. Hesse, M. Alexe, *J. Appl. Phys.* **2010**, *107*, 084111.
[18] J. Li, Z. Liu, B. W. Wessels, *J. Appl. Phys.* **2010**, *107*, 124106.
[19] A. K. Jonscher, *Universal Relaxation Law*, Chelsea Dielectrics Press, London, UK **1996**.
[20] a) W. J. Merz, *Phys. Rev.* **1954**, *95*, 690; b) E. Fatuzzo, W. J. Merz, *Phys. Rev.* **1959**, *116*, 61.
[21] M. Molotskii, *J. Appl. Phys.* **2000**, *88*, 5318.
[22] K. B. Chong, F. Guiu, M. J. Reece, *J. Appl. Phys.* **2008**, *103*, 014101.
[23] S. Jesse, B. J. Rodriguez, S. Choudhury, A. P. Baddorf, I. Vrejoiu, D. Hesse, M. Alexe, E. A. Eliseev, A. N. Morozovska, J. Zhang, L.-Q. Chen, S. Kalinin, *Nat. Mater.* **2008**, *7*, 209.
[24] S. Hashimoto, H. Orihara, Y. Ishibashi, *J. Phys. Soc. Jpn.* **1994**, *63*, 1601.
[25] O. Lohse, M. Grossmann, U. Boettger, D. Bolten, R. Waser, *J. Appl. Phys.* **2001**, *89*, 2332.
[26] T. M. Kamel, F. X. N. M. Kools, G. de With, *J. Eur. Ceram. Soc.* **2007**, *27*, 2471.
[27] F. Preisach, *Z. Phys.* **1935**, *94*, 277.
[28] G. Robert, D. Damjanovic, N. Setter, A. V. Turik, *J. Appl. Phys.* **2001**, *89*, 5067.
[29] K. Seal, S. Jesse, M. P. Nikiforov, S. V. Kalinin, I. Fujii, P. Bintachitt, S. Trolier-McKinstry, *Phys. Rev. Lett.* **2009**, *103*, 057601.
[30] S. V. Kalinin, B. J. Rodriguez, J. D. Budai, S. Jesse, A. N. Morozovska, A. A. Bokov, Z.-G. Ye, *Phys. Rev. B* **2010**, *81*, 064107.
[31] M. V. Feigel'man, V. B. Geshkenbein, A. I. Larkin, V. M. Vinokur, *Phys. Rev. Lett.* **1989**, *63*, 2303.
[32] N. Uchida, T. Ikeda, *Jpn. J. Appl. Phys.* **1967**, *6*, 1079.
[33] T. Furukawa, *Phase Trans.* **1989**, *18*, 143.
[34] A. B. Migdal, *Qualitative Methods in Quantum Theory*, Westview Press, Boulder, CO **2000**.
[35] H. Kungl, M. J. Hoffmann, *J. Appl. Phys.* **2010**, *107*, 054111.
[36] M. Ehmke, J. Glaum, W. Jo, T. Granzow, J. Rödel, *J. Am. Ceram. Soc.* **2011**, *94*, 2473.
[37] T. Furukawa, *IEEE Trans. Dielectr. Electr. Insul.* **1989**, *24*, 375.
[38] T. Furukawa, M. Date, G. E. Johnson, *J. Appl. Phys.* **1983**, *54*, 1540.
[39] T. Mitsui, in *Springer Handbook of Condensed Matter and Materials Data*, (Eds: W. Martienssen, H. Warlimont), Springer, Berlin, Germany **2005**, Ch. 4.5.
[40] J. Rödel, W. Jo, K. T. P. Seifert, E. M. Anton, T. Granzow, D. Damjanovic, *J. Am. Ceram. Soc.* **2009**, *92*, 1153.
[41] T. Takenaka, K. Maruyama, K. Sakata, *Jpn. J. Appl. Phys.* **1991**, *30*, 2236.
[42] W. Jo, S. Schaab, E. Sapper, L. A. Schmidt, H.-J. Kleebe, A. J. Bell, J. Rödel, *J. Appl. Phys.* **2011**, *110*, 074106.
[43] H. Onozuka, Y. Kitanaka, Y. Noguchi, M. Miyayama, *Jpn. J. Appl. Phys.* **2011**, *50*, 09NE07.
[44] P. Sharma, T. J. Reece, S. Ducharme, A. Gruverman, *Nano Lett.* **2011**, *11*, 1970.
[45] C. Jullian, J. F. Li, D. Viehland, *J. Appl. Phys.* **2004**, *95*, 5671.
[46] I. Stolichnov, A. K. Tagantsev, E. Colla, N. Setter, *J. Appl. Phys.* **2005**, *98*, 084106.
[47] A. V. Bune, V. M. Fridkin, S. Ducharme, S. G. Yudin, L. M. Blinov, S. P. Palto, A. V. Sorokin, A. Zlatkin, *Nature* **1998**, *391*, 874.
[48] L. Zhang, *EPL* **2010**, *91*, 47001.
[49] J. F. Scott, *Adv. Mater.* **2010**, *22*, 5315.
[50] X. Chen, O. Sichelschmidt, W. Kleemann, O. Petracic, C. Binek, J. B. Sousa, C. Cardoso, P. P. Freitas, *Phys. Rev. Lett.* **2002**, *89*, 137203.
[51] D. Kedzierski, E. V. Kirichenko, V. A. Stephanovich, *Phys. Lett. A* **2011**, *375*, 685.
[52] R. H. Koch, G. Grinstein, G. A. Keefe, Y. Lu, P. L. Trouilloud, W. J. Gallagher, S. S. P. Parkin, *Phys. Rev. Lett.* **2000**, *84*, 5419.